An explanation for the sister repulsion phenomenon in Patterson's *f*-statistics

Gözde Atağ,[1,2,*] Shamam Waldman,[3] Shai Carmi (ID),[4] Mehmet Somel (ID) [1,*]

[1]Department of Biological Sciences, Middle East Technical University, Ankara 06800, Turkey
[2]Department of Evolutionary Genetics, Max Planck Institute for Evolutionary Anthropology, Leipzig 04103, Germany
[3]Department of Human Evolutionary Biology, Harvard University, Cambridge, MA 02138, USA
[4]Braun School of Public Health and Community Medicine, The Hebrew University of Jerusalem, Jerusalem 9112102, Israel

*Corresponding author: Department of Biological Sciences, Middle East Technical University, Ankara 06800, Turkey. Email: atag.gozde@gmail.com; *Corresponding author: Department of Biological Sciences, Middle East Technical University, Ankara 06800, Turkey. Email: somel.mehmet@gmail.com

Patterson's *f*-statistics are among the most heavily utilized tools for analyzing genome-wide allele frequency data for demographic inference. Beyond studying admixture, *f*₃- and *f*₄-statistics are also used for clustering populations to identify groups with similar histories. However, previous studies have noted an unexpected behavior of *f*-statistics: multiple populations from a certain region systematically show higher genetic affinity to a more distant population than to their neighbors, a pattern that is mismatched with alternative measures of genetic similarity. We call this counter-intuitive pattern "sister repulsion". We first present a novel instance of sister repulsion, where genomes from Bronze Age East Anatolian sites show higher affinity toward Bronze Age Greece rather than each other. This is observed both using *f*₃- and *f*₄-statistics, contrasts with archaeological/historical expectation, and also contradicts genetic affinity patterns captured using principal components analysis or multidimensional scaling on genetic distances. We then propose a simple demographic model to explain this pattern, where sister populations receive gene flow from a genetically distant source. We calculate *f*₃- and *f*₄-statistics using simulated genetic data with varying population genetic parameters, confirming that low-level gene flow from an external source into populations from 1 region can create sister repulsion in *f*-statistics. Unidirectional gene flow between the studied regions (without an external source) can likewise create repulsion. Meanwhile, similar to our empirical observations, multidimensional scaling analyses of genetic distances still cluster sister populations together. Overall, our results highlight the impact of low-level admixture events when inferring demographic history using *f*-statistics.

Keywords: demographic inference; *f*-statistics; admixture; deep ancestry; ancient DNA

Introduction

Over the last decade, Patterson's *f*-statistics (Patterson *et al.* 2012) have become one of the most commonly applied tools in population genetics studies involving the analysis of genome-wide data. Various *f*-statistics (*f*₂, outgroup-*f*₃, admixture-*f*₃, and *f*₄) quantify divergence, shared genetic drift, and treeness among populations by comparing allele frequencies. These measurements enable the identification of population structure, differentiation, and admixture events and help decipher the demographic history of the studied populations (Peter 2016, 2022; Harris and DeGiorgio 2017; Lipson 2020). The description of *f*-statistics as being robust to heterogeneity of sample size/coverage and ascertainment biases (Patterson *et al.* 2012) has gained them high popularity.

The outgroup-*f*₃-statistics in the form of *f*₃(*Outgroup; Pop2, Pop3*) measures shared drift between *Pop2* and *Pop3* relative to an outgroup, and its magnitude has been used as a measure of pairwise population affinity. The *f*₄-statistic measures treeness, such that *f*₄(*Outgroup, Pop1; Pop2, Pop3*) is expected to be 0 if *Pop1* shares the same amount of drift with *Pop2* and *Pop3*, i.e. *Pop1* is a real

outgroup to the latter 2 populations. Significant deviation from 0 can be interpreted as evidence for admixture (Patterson *et al.* 2012), but the *f*₄-statistic can also be used for studying population structure and shared demographic histories. If *Pop2* and *Pop3* share more of their demographic history with each other than they do with *Pop1*, i.e. shared drift and/or similar admixture events that *Pop1* did not experience, and if there is no post-split admixture, we expect *f*₄(*Outgroup, Pop1; Pop2, Pop3*) to be nonsignificant, while *f*₄(*Outgroup, Pop2; Pop1, Pop3*) and *f*₄(*Outgroup, Pop3; Pop1, Pop2*) to both be positive. Gene flow from *Pop1* into *Pop3* in the same model will also cause *f*₄(*Outgroup, Pop1; Pop2, Pop3*) to be positive. Thus, in addition to testing admixture, reciprocal affinity in *f*₄-tests has frequently been used as a tool for clustering populations based on allele frequency similarities, where clustering implies similar histories. The outgroup-*f*₃-statistics has similarly been used to evaluate shared history between populations.

Nevertheless, *f*-statistics are not always straightforward to interpret. Complications of diverse types and origins have been noted, such as possible misinterpretation of an outgroup as an

admixture source when using admixture-f_3 (Patterson *et al.* 2012), or the sensitivity of f_4-statistics to SNP ascertainment schemes as showcased for demographic modeling of African human populations using SNPs identified in non-African groups (Bergström *et al.* 2020; Flegontov *et al.* 2023). The most widespread type of issue arguably involves the interpretation of f_4-statistics under the assumption of a simple demographic model where the real history is substantially more complicated. For instance, unrecognized genetic structure can be misinterpreted as admixture events (Slatkin and Pollack 2008; Durand *et al.* 2011; Eriksson and Manica 2012). A similar confounding effect can be created by backward gene flow, as shown for Neanderthal admixture estimates varying spuriously over time due to African gene flow into Eurasia (Petr *et al.* 2019a).

Previous work using *f*-statistics has noted another unexpected pattern that has yet remained largely unexplored, to our knowledge. Using f_4-statistics, Kılınç *et al.* (2017) observed higher affinity of all Anatolian Neolithic groups to a Neolithic genome from Greece than to each other, a pattern that appeared difficult to interpret. Even more surprising was the observation that modern-day North African populations showed higher affinity to modern-day Sardinians than to each other using f_3- and f_4-statistics (Rodríguez-Varela *et al.* 2017). This pattern was hypothesized to stem from gene flow from sub-Saharan Africa into North Africa, but the case was not studied further.

Here, we provide another case of this pattern, which we call "sister repulsion", by comparing genomes from the Bronze Age (BA) East Mediterranean. We then describe a simple theoretical model that can explain this effect, propose different scenarios involving external and regional gene flow to explain sister repulsion, and recapitulate the observed *f*-statistics using simulations under these models, with various parameter values. Our results showcase how complex demographic histories can lead to counterintuitive patterns of f_3- and f_4-statistics when used for studying shared population history.

Results and discussion

Our initial motivation was to investigate population structure and admixture patterns in the East Mediterranean during the Bronze Ages, a period which saw population growth and extensive interregional trade networks being established, as inferred from material culture data (Şahoğlu 2005; Kouka 2016; Massa 2016). We studied genetic affinities between published genomic data from $n = 6$ BA populations from the region of modern-day Greece (2400–1070 BCE) (henceforth Greece) and $n = 5$ populations from BA East Anatolia (3700–1303 BCE) (Lazaridis *et al.* 2017, 2022; Skourtanioti *et al.* 2020) (Supplementary Table 1, Supplementary Fig. 2).

First, we explored genetic clustering among populations with principal components analysis (PCA) and multidimensional scaling (MDS) analysis. In the PCA, where the ancient genomes are projected on a PC space calculated from modern-day West Eurasians, ancient genomes from Greece cluster separately from those from East Anatolia (Supplementary Fig. 1). Then, we calculated the genetic distance between all pairs of populations using 1-f_3(*Yoruba; Pop1, Pop2*) to represent the distance between populations *Pop1* and *Pop2*. Applying MDS analysis on the resulting pairwise distance matrix (Fu *et al.* 2016), the populations showed a tendency to cluster by region in MDS space, i.e. Greece and Anatolia separated along Coordinate 1 (Fig. 1a and b).

Intriguingly, f_3-statistics revealed a counter-intuitive trend. In contrast to the patterns observed in PCA and MDS, the values

f_3(*Yoruba; EAnatoliaY, GreeceX*) were consistently higher than the values f_3(*Yoruba; EAnatoliaY, EAnatoliaZ*), where *GreeceX* is 1 of the 6 populations from Greece, while *EAnatoliaY* and *EAnatoliaZ* are any of the 5 populations from East Anatolia (Fig. 1b–e, and g, Supplementary Table 2). At face value, this would imply more similar histories between any East Anatolian population with those from Greece than other neighboring East Anatolian populations. Plotting the genetic vs geographic distances, we observed a lack of correlation within the East Anatolian populations (Fig. 1f).

We next calculated f_4-statistics of the form f_4(*Yoruba, AnatoliaY; AnatoliaZ, GreeceX*). In 99% of 120 comparisons, we observed positive values (42% significant at Z > 3, without correcting for multiple testing) (Fig. 1d, Supplementary Table 3). No f_4-statistic was significantly negative, i.e. no East Anatolian group significantly shared more drift with 1 of its neighbors over a population from Greece. This starkly contrasts with the expected geographical and genetic clustering [given multiple observations of spatial population structure in ancient humans (e.g. Altınışık *et al.* 2022; Antonio *et al.* 2024)], while it does mirror the outgroup-f_3 results.

We then asked whether population or time structure within the 2 regional groups could be behind this pattern, as the sampled individuals span several thousands of years. We investigated this using f_4-statistics within 1 site in East Anatolia, Alalakh. We randomly split the $n = 25$ genomes from Alalakh into 2 groups and calculated f_4(*Yoruba, Group1; Group2, Greece*), 10 times independently. We observed positive f_4 values, or sister repulsion, in all 10 Alalakh replicates (all f_4 values were significant except for 1 trial) (Supplementary Table 4).

Assuming this sister repulsion pattern is not caused by technical artifacts, such as contamination, we might imagine 2 explanations. One may be gene flow from modern-day Greece into different East Anatolian populations or the ancestors of all East Anatolian populations. An alternative explanation and a possibly more likely scenario could involve admixture from an external and diverse source impacting East Anatolia. This would be similar to that hypothesized by Rodríguez-Varela *et al.* (2017) and analogous to the "outgroup case" described by Patterson *et al.* (2012).

The ancestral components of both Anatolia and Greek Early/Middle Bronze Age genomes comprise Neolithic Anatolia and eastern-related ancestry from Caucasus/Mesopotamia (Clemente *et al.* 2021; Lazaridis *et al.* 2022; Skourtanioti *et al.* 2023). We hypothesized that additional external gene flow into East Anatolia (e.g. from sources such as the Levant, Zagros, or Mesopotamia) that BA populations from Greece did not receive could lead to differentiation within the former region and might explain the observed sister repulsion pattern. As a first test of this idea, we calculated intra-regional diversity within each site, using the pairwise statistic 1 – outgroup-f_3 among genomes within a site as the diversity measure. This revealed significantly higher median diversity in BA East Anatolia than in BA Greece (Wilcoxon rank sum test $P = 3e^{-09}$, Fig. 1c, Supplementary Fig. 3).

This supports the hypothesis that gene flow from a divergent source (so-called "deep ancestry") might explain this pattern. We investigated the idea further using the demographic scenario described in Fig. 2. We define A and B as 2 sister populations, X as a more distant lineage, Z as the source of external gene flow into A and B, and O as outgroup to all. Here, A, B, and X represent our focal populations; A and B could represent 2 BA East Anatolian groups, X could be a BA population from the region of modern-day Greece, and Z would be an unknown, distant source that admixes only with East Anatolia. The ancestors of multiple populations are denoted by their merged names (i.e. the ancestor population of A
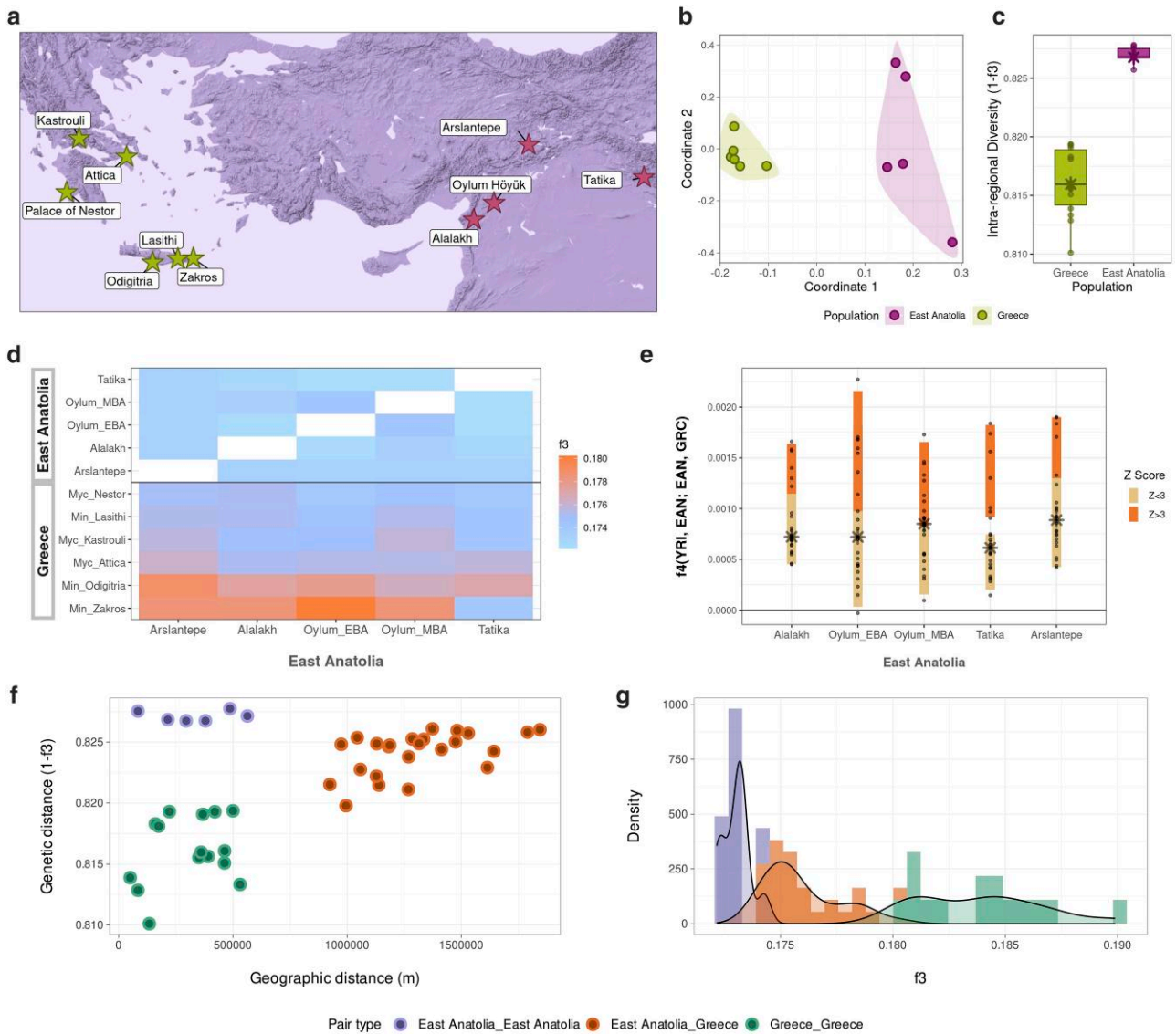
Fig. 1. a) Geographical distribution of the studied Bronze Age genomes from the regions of modern-day Greece and East Anatolia. b) Genetic clustering of the populations in line with geography revealed by multidimensional scaling (MDS) analysis, using $1 -$ outgroup-f_3 values as genetic distances. Supplementary Fig. 1 also presents a PCA, which also shows the absence of visible structure in these gene pools. c) Intra-regional diversity of the populations measured as pairwise $1 -$ outgroup-f_3 values within regions. Each point represents comparisons of settlements from the same region. d) f_3-Statistics of the form $f_3(Yoruba; East Anatolia, X)$ where X corresponds to populations from Greece and East Anatolia. The x-axis shows East Anatolian populations while the y-axis shows Greece and East Anatolia. e) f_4-Statistics of the form $f_4(Yoruba, East Anatolia; East Anatolia, Greece)$, where positive values depict higher affinity of BA East Anatolian populations toward contemporary populations from Greece. f) Geographic vs genetic distances (1-f_3) between and within regions. g) Distribution of f_3 values between and within regions.

and B is called AB). Note that in the model, A and B are sisters, with the same demographic histories.
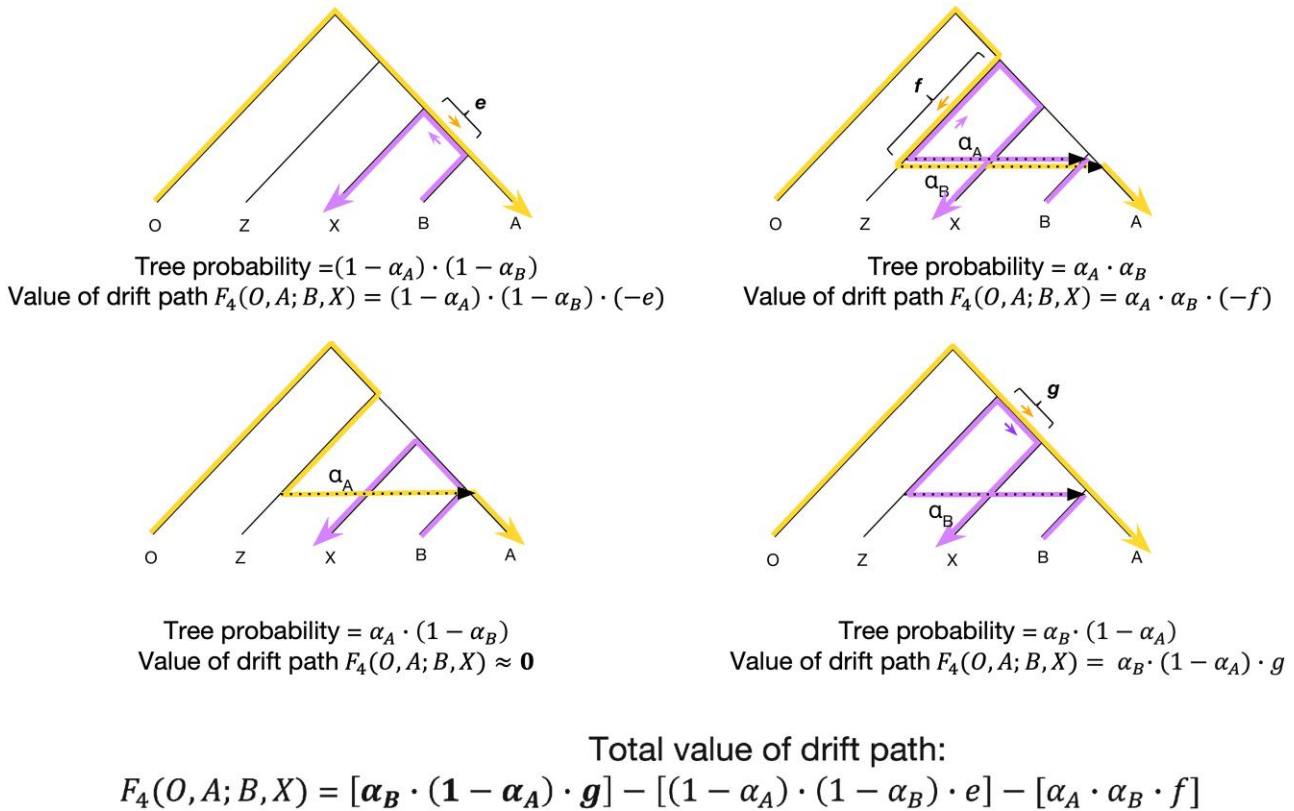
We studied the theoretical conditions for the expected value of $F_4(O, A; B, X)$ to be positive in this model (we follow Patterson *et al.* in using upper case letters for expected values). The F_4-statistic can be decomposed into the sum of overlapping drift paths between O to A and B to X. Under gene flow from Z into A and/or B, there emerge 4 alternative drift paths, described in Fig. 3. These depend on α_A and α_B, the probabilities of gene flow (admixture proportions) from Z into A and B. The expected F_4 is the weighted sum of the values of these paths. One of these paths produces a positive value, i.e. sister repulsion, which depends on the branch length g separating Z from the common ancestor of A, B, and X (branch ABX in Fig. 2), on the branch length e separating X from the common ancestor of A and B (branch AB in Fig. 2) and also on the admixture proportions

α_A and α_B. Note that the branch lengths represent drift and will be a function of time and N_e.

Now let us assume that the admixture proportions in A and B are the same ($\alpha_A = \alpha_B$) and small, so that α^2 is negligible and $1 - \alpha$ is close to 1. Then, $g \cdot \alpha > e$ would fulfill the condition of a positive F_4, i.e. sister repulsion. For instance, consider a simplistic scenario where all populations had the same Ne and the same admixture proportions. If BA populations from the regions of modern-day Greece and E Anatolia had split from their common ancestor 30 generations before sampling (~900 years), and then received gene flow from a population that had split 2,000 generations before sampling (~60,000 years), an admixture proportion of (2000-30)/900, ~0.02, would suffice to create a positive F_4 value. Gene flow into the common ancestor of A and B could also lead to positive F_4 (Supplementary Fig. 9). This is in line with our
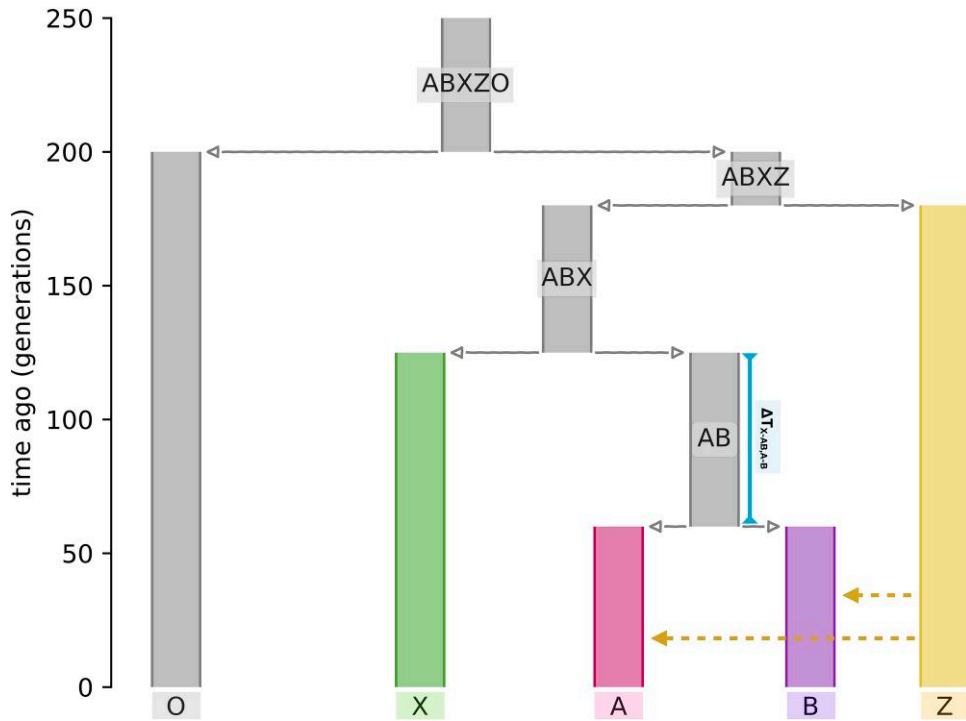
Fig. 2. Demographic model used for the population genetic simulations. The ancestral populations are named as combinations of the descending population names. Population O is the outgroup used in the calculation of *f*-statistics. Dashed lines represent equal rates of continuous migration from Z to A and B per generation after the split between A and B and the present day. The vertical line on the right side of the AB branch corresponds to the parameter $\Delta T_{X\text{-}AB,A\text{-}B}$.

Tree probability $=(1 - \alpha_A) \cdot (1 - \alpha_B)$
Value of drift path $F_4(O, A; B, X) = (1 - \alpha_A) \cdot (1 - \alpha_B) \cdot (-e)$

Tree probability $= \alpha_A \cdot \alpha_B$
Value of drift path $F_4(O, A; B, X) = \alpha_A \cdot \alpha_B \cdot (-f)$

Tree probability $= \alpha_A \cdot (1 - \alpha_B)$
Value of drift path $F_4(O, A; B, X) \approx 0$

Tree probability $= \alpha_B \cdot (1 - \alpha_A)$
Value of drift path $F_4(O, A; B, X) = \alpha_B \cdot (1 - \alpha_A) \cdot g$

Total value of drift path:

$$F_4(O, A; B, X) = [\boldsymbol{\alpha_B \cdot (1 - \alpha_A) \cdot g}] - [(1 - \alpha_A) \cdot (1 - \alpha_B) \cdot e] - [\alpha_A \cdot \alpha_B \cdot f]$$

Fig. 3. Expected F_4 values under distant admixture. The 4 trees with arrows show 4 possible drift paths that can contribute to $F_4(O, A; B, X)$. Here, sister populations A or B have independently received gene flow (dashed arrow) from the distant branch Z with admixture proportions α_A and α_B, respectively, after their split from each other. The probability of each path and its value as a product of its probability and the drift magnitude (indicated by letters *e*, *f*, and *g*) are shown below each tree. The expected average F_4 value (Patterson *et al.* 2012) is shown at the bottom, with the positive component in bold. The small arrows indicate the direction of the drift paths from O → A and B → X, which determine the sign of that F_4 path.

Table 1. Parameter values used for the main population genetic simulations.

Parameter	Values	Definition
$m_{Z \to A,B}$	0, 0.001, 0.005, 0.01, 0.1	Migration rate from Z to A and B
Ne_Z	5 k, 15 k, 35 k	Effective population size of source Z
Ne_{AB}	5 k, 15 k, 35 k	Effective population size of ancestral AB
Ne_{ABX}	1 k, 3 k, 5 k	Effective population size of ancestral ABX
T_{A-B}	30, 60, 90	Divergence time of A and B
T_{X-AB}	100, 125, 150	Divergence time of X and AB
$\Delta T_{X-AB,A-B}$	10, 65, 120	Difference between T_{A-B} and T_{X-AB}
Ne_X[a]	1 k, 3 k, 5 k	Effective population size of X
$m_{X \to A,B}$[a]	0, 0.001, 0.005, 0.01, 0.1	Migration rate from X to A and B

Migration rates are given per generation, divergence times are given in generations.

[a]The given parameter values for Ne_X and $m_{X \to A,B}$ were tested only for scenarios where $Ne_{ABX} = 1$ k and $\Delta T_{X-AB,A-B} = 65$. In the remaining scenarios, Ne_X was fixed at 5 k and $m_{X \to A,B}$ at 0.

observation that random subsets of BA Alalakh individuals also show sister repulsion (Supplementary Note 1).

Our model thus suggests that sister repulsion is theoretically possible. This motivated us to further study how *f*-statistics would behave numerically in a demographic model akin to the case study, and specifically to investigate how different parameter values of the model and their combinations would affect the sister repulsion outcome, also in the face of continuous gene flow. We thus ran population genetic simulations using msprime v1.0 (Baumdicker *et al.* 2022) under the same general model in Fig. 2 and assessed the effect of each parameter in depth. Specifically, we varied the parameters $m_{Z \to A,B}$, Ne_Z, Ne_{AB}, Ne_{ABX}, T_{A-B}, and T_{X-AB} (Table 1). The continuous migration $m_{Z \to A,B}$ was set to start subsequent to the A-B split. In each case, we sampled 25 genomes each from O, X, A, and B, and calculated various outgroup-f_3- and f_4-statistics.

In this model (Fig. 2), one would naively anticipate $f_4(O, A; B, X)$ values to be negative since the populations A and B share more similar overall histories with each other than with X, as in tree A in Fig. 3. Indeed, in the absence of gene flow from Z into A/B ($m = 0$), f_4-statistics are nearly always negative, reflecting higher shared drift between A and B than with X (Fig. 4, Supplementary Fig. 2). However, f_4 values change as we allow migration from Z into A/B (from $m = 0$ to $m = 0.1$), although in nonlinear fashion. When we increased migration from 0 to 0.01, we observed a monotonic rise in $f_4(O, A; B, X)$ values, i.e. an increasing trend toward sister repulsion (Fig. 4). Under specific conditions, e.g. $Ne_{ABX} = 1$k, $0.001 \le m < 0.1$ and $\Delta T_{X-AB,A-B} = 10$, all $f_4(O, A; B, X)$ values were positive (Fig. 4, Supplementary Fig. 4). We then calculated 1-f_3 based MDS and intra-regional diversities, and observed that A and B clustered separately from X, and also had higher diversity than X (Supplementary Fig. 5; Supplementary Note 2). These patterns are analogous to that observed in the empirical data where 2 East Anatolian populations showed higher affinity to populations from Greece than to each other (Fig. 1). In summary, we can replicate the empirical result effectively under specific conditions.

We note several conditions driving more positive $f_4(O, A; B, X)$ values under low-level migration in our model (Fig. 4, Supplementary Fig. 6; Table 1).

- Low $\Delta T_{X-AB,A-B}$: this means A and B share less drift relative to X (the phylogeny is more star-like). Also, because T_{AB-X} is fixed in the model, low $\Delta T_{X-AB,A-B}$ leads to T_{A-B} going back in time (Fig. 2) and therefore A and B each being impacted by Z-sourced continuous migration for additional generations (i.e. larger α in Fig. 3).
- Low Ne_{ABX}: this causes higher shared drift between A, B, and X (i.e. larger g in Fig. 3).
- High Ne_{AB}: this leads to lower shared drift between A and B (i.e. smaller e in Fig. 3).
- High Ne_Z: this causes Z to be subject to less drift, such that the negative branch length f in Fig. 3 becomes smaller in magnitude.

Next, we studied the phenomenon with additional scenarios (Supplementary Figs. 7–13, Supplementary Note 2). Scenarios involving asymmetric gene flow into B vs A (Supplementary Fig. 7) and gene flow into the ancestral population AB rather than A and B separately (Supplementary Figs. 8 and 9) yielded similar results to our original set up. We also found that instead of an external population Z, gene flow from X also leads to positive f_4 values (Supplementary Fig. 13). In simulations where we randomly split a single population we again found positive f_4 values (Supplementary Table 5).

These results reveal how various demographic scenarios can lead to sister repulsion, i.e. closely related pairs of populations (A and B) showing higher affinity to a lineage that has split earlier from them (X) in f_3- and f_4-statistics. In particular, low-level gene flow from an external source (Z) into A and B or their common ancestor may frequently explain empirical cases of sister repulsion. We note that the repulsion effect happens because the *f*-statistics are point estimates that represent the average across diverse phylogenetic paths in a population's demographic history. In our model, the effect depends on the distance of Z to XAB; therefore the introduction of so-called "deep ancestry" can readily shift the expected values. This also resembles the "ghost admixture" phenomenon when gene flow from distant sources can bias phylogenetic inference (Rogers and Bohlender 2015; Tricou *et al.* 2022).

In the scenarios studied, A and B share more similar demographic histories with each other than with X, although this is not directly reflected in the f_3- and f_4-statistics. As a quick diagnostic of the problem, we highlight the method of randomly splitting 1 of the target populations, whereby if f_4-statistics show the repulsion signal between the 2 subgroups, sister repulsion is evident. When sister repulsion is suspected, researchers may resort to alternative tools such as genetic clustering (e.g. MDS), qpAdm modeling (Harney *et al.* 2021) or using time stratified variants to disentangle the signals. Researchers may further be interested in evaluating whether post-split admixture from X or an external population Z is more likely, which may be evaluated using additional sources of information, such as local ancestry inference or archaeological/historical evidence for regional gene flow. In the empirical cases we covered, such as sister repulsion in Bronze Age East Anatolia, external gene flow from genetically distant populations (e.g. related to sub-Saharan Africa) may be a more parsimonious explanation than direct gene flow from the population being compared (e.g. Greece).

Methods
Ancient genomes
We used 79 published Bronze Age genomes from the East Mediterranean (Supplementary Table 1), from a publicly available dataset comprising the ancient individuals analyzed in Lazaridis *et al.* 2022, genotyped at the 1240K SNP positions (Lazaridis *et al.* 2022).
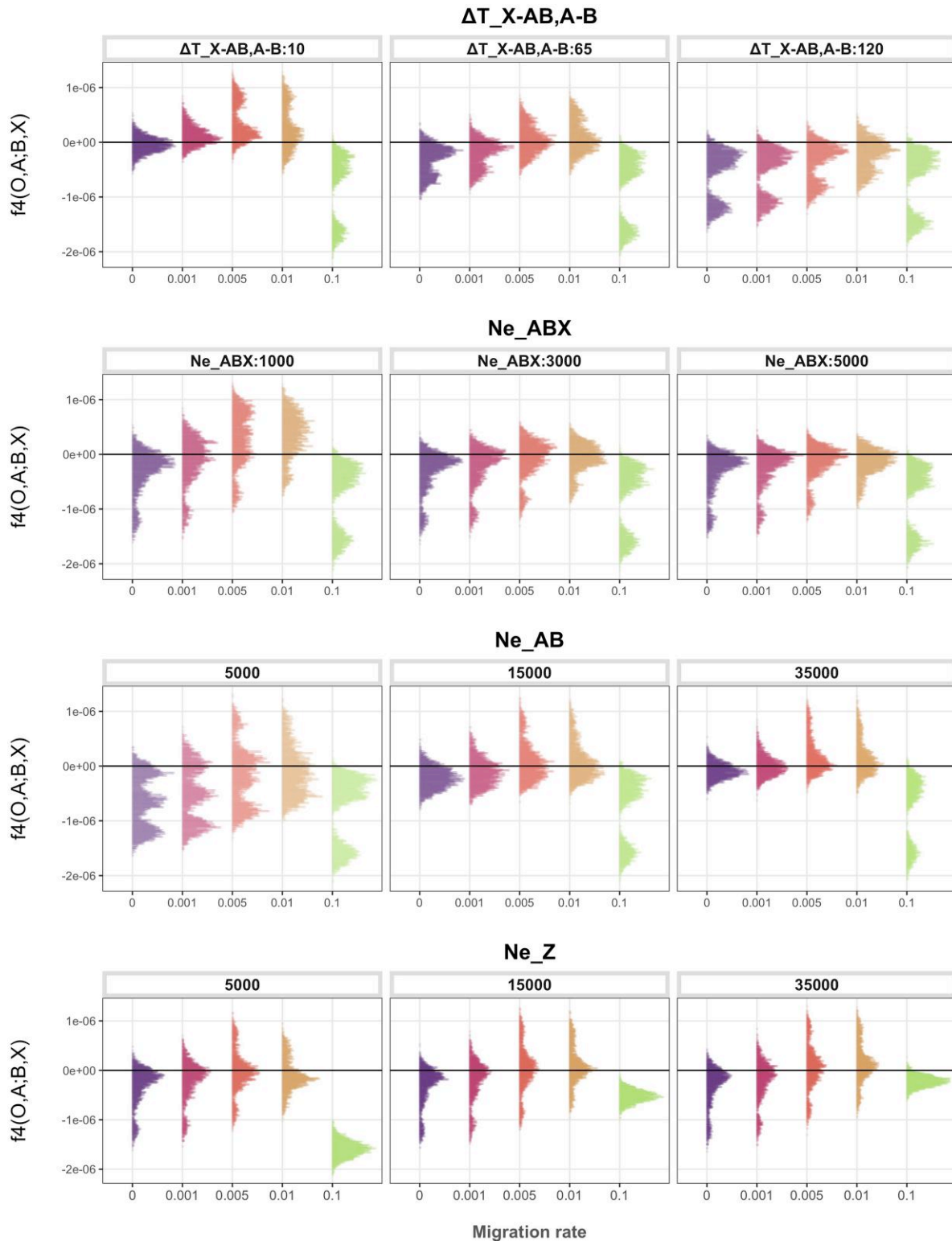
Fig. 4. Change in f_4-statistics of the form $f_4(O, A; B, X)$ depending on the varying parameters in population genetic simulations, where negative values represent higher affinity between A and B, and positive values higher affinity between A and X. The panels for each parameter contain all values of the remaining studied parameters and are explained in Table 1. The multimodality arises because each distribution is collected from a range of simulations run under a range of parameters with diverse effects on the f_4-statistics.

PCA

For the PCA, we used the Human Origins Dataset (Lazaridis *et al.* 2014, 2016), containing 2,583 present-day genomes genotyped at the Affymetrix Human Origins Array positions, merged with the

Bronze Age genomes. PCA was performed using smartpca v.18140, with option lsqproject:YES, implemented in EIGENSOFT v.7.2.0 (Patterson et al. 2006). We projected the ancient individuals onto the first 2 principal components calculated from present-day

Western Eurasian diversity based on populations from the Human Origins panel.

f₃- and *f₄*-statistics and MDS

We calculated outgroup-*f₃*- and *f₄*-statistics using admixr v0.9.1, which runs AdmixTools v.7.0.2, with default parameters (Patterson *et al.* 2012; Petr *et al.* 2019b). Within-group genetic diversities were estimated by computing pairwise $1 - \text{outgroup-}f_3$. All statistics were computed based on the 1240K dataset, using 3 modern-day Yoruba individuals as the outgroup. We estimated pairwise genetic distances with $1 - \text{outgroup-}f_3$, computed a distance matrix of $1\text{-}f_3$ values, and performed a classical MDS analysis using the cmdscale algorithm implemented in the R package stats (R Core Team 2023).

The geodesic distances between sites for the comparison of genetic vs geographic distances were calculated using the R package geosphere (Hijmans 2010).

For the calculation of $f_4(\text{Yoruba, Group1; Group2, Greece})$ statistics within the East Anatolian site Alalakh, we randomly split the 25 individuals in 2 groups of 20 and 5 and 15 and 10. Repeating each of the 2 groupings 5 times, we computed 10 f_4-statistics in total.

Simulations

We used msprime v1.0 (Baumdicker *et al.* 2022) to simulate diploid sequences of 100 Mb, where we sampled 25 individuals from each population. The mutation rate and the recombination rate were chosen as $1e^{-8}$ and $1.1e^{-8}$ per generation, respectively. Each scenario had 100 replicates, varying the parameters in Table 1. The outgroup-*f₃*- and f₄-statistics were calculated using tskit v0.5.6. Additional information can be found in Supplementary Note 3.

Data availability

The code and parameters for generating the simulated data, and all other scripts used in the study, are deposited under https://github.com/goztag/msprime_fstats/tree/main.

Supplemental material available at GENETICS online.

Conflicts of interest

The author(s) declare no conflicts of interest.

Literature cited

Altınışık NE, Kazancı DD, Aydoğan A, Gemici HC, Erdal ÖD, Sarıaltun S, Vural KB, Koptekin D, Gürün K, Sağlıcan E, *et al.* 2022. A genomic snapshot of demographic and cultural dynamism in Upper Mesopotamia during the Neolithic Transition. Sci Adv. 8(44): eabo3609. doi:10.1126/sciadv.abo3609.

Antonio ML, Weiß CL, Gao Z, Sawyer S, Oberreiter V, Moots HM, Spence JP, Cheronet O, Zagorc B, Praxmarer E, *et al.* 2024. Stable population structure in Europe since the Iron Age, despite high mobility. eLife. 13:e79714. doi:10.7554/elife.79714.

Baumdicker F, Bisschop G, Goldstein D, Gower G, Ragsdale AP, Tsambos G, Zhu S, Eldon B, Ellerman EC, Galloway JG, *et al.* 2022. Efficient ancestry and mutation simulation with msprime 1.0. Genetics. 220(3):iyab229. doi:10.1093/genetics/iyab229.

Bergström A, McCarthy SA, Hui R, Almarri MA, Ayub Q, Danecek P, Chen Y, Felkel S, Hallast P, Kamm J, *et al.* 2020. Insights into human genetic variation and population history from 929 diverse genomes. Science. 367(6484):eaay5012. doi:10.1126/science.aay5012.

Clemente F, Unterländer M, Dolgova O, Amorim CEG, Coroado-Santos F, Neuenschwander S, Ganiatsou E, Cruz Dávalos DI, Anchieri L, Michaud F, *et al.* 2021. The genomic history of the Aegean palatial civilizations. Cell. 184(10):2565–2586.e21. doi:10.1016/j.cell.2021.03.039.

Durand EY, Patterson N, Reich D, Slatkin M. 2011. Testing for ancient admixture between closely related populations. Mol Biol Evol. 28(8):2239–2252. doi:10.1093/molbev/msr048.

Eriksson A, Manica A. 2012. Effect of ancient population structure on the degree of polymorphism shared between modern human populations and ancient hominins. Proc Natl Acad Sci U S A. 109(35): 13956–13960. doi:10.1073/pnas.1200567109.

Flegontov P, Işıldak U, Maier R, Yüncü E, Changmai P, Reich D. 2023. Modeling of African population history using f-statistics is biased when applying all previously proposed SNP ascertainment schemes. PLoS Genet. 19(9):e1010931. doi:10.1371/journal.pgen.1010931.

Fu Q, Posth C, Hajdinjak M, Petr M, Mallick S, Mittnik A, Nickel B, Peltzer A, Rohland N, Slon V, *et al.* 2016. The genetic history of Ice Age Europe. Nature. 534(7606):200–205. doi:10.1038/nature17993.

Harney É, Patterson N, Reich D, Wakeley J. 2021. Assessing the performance of qpAdm: a statistical tool for studying population admixture. Genetics. 217(4):iyaa045. doi:10.1093/genetics/iyaa045.

Harris AM, DeGiorgio M. 2017. Admixture and ancestry inference from ancient and modern samples through measures of population genetic drift. Hum Biol. 89(1):21–46. doi:10.13110/humanbiology.89.1.02.

Hijmans RJ. 2010. geosphere: Spherical Trigonometry. R package version 1.5-18, https://cran.r-project.org/web/packages/geosphere.

Kılınç GM, Koptekin D, Atakuman Ç, Sümer AP, Dönertaş HM, Yaka R, Bilgin CC, Büyükkarakaya AM, Baird D, Altınışık E, Yaka R, Bilgin CC, Büyükkarakaya AM, Baird D, Altınışık E, *et al.* 2017. Archaeogenomic analysis of the first steps of Neolithization in Anatolia and the Aegean. Proc R Soc Lond B Biol Sci. 284(1867): 20172064. doi:10.1098/rspb.2017.2064.

Kouka O. 2016. The built environment and cultural connectivity in the Aegean Early Bronze Age. In: Molloy BPC, editors. Of Odysseys and Oddities, Sheffield Studies in Aegean Archaeology. Oxford, UK: Oxbow Books. p. 203–222.

Lazaridis I, Alpaslan-Roodenberg S, Pinhasi R, Reich D. 2022. The genetic history of the Southern Arc: a bridge between West Asia and Europe. Harvard Dataverse. V1. doi:10.7910/DVN/3AR0CD.

Lazaridis I, Mittnik A, Patterson N, Mallick S, Rohland N, Pfrengle S, Furtwängler A, Peltzer A, Posth C, Vasilakis A, *et al.* 2017. Genetic origins of the Minoans and Mycenaeans. Nature. 548(7666):214–218. doi:10.1038/nature23310.

Lazaridis I, Nadel D, Rollefson G, Merrett DC, Rohland N, Mallick S, Fernandes D, Novak M, Gamarra B, Sirak K, *et al.* 2016. Genomic

insights into the origin of farming in the ancient Near East. Nature. 536(7617):419–424. doi:10.1038/nature19310.

Lazaridis I, Patterson N, Mittnik A, Renaud G, Mallick S, Kirsanow K, Sudmant PH, Schraiber JG, Castellano S, Lipson M, *et al.* 2014. Ancient human genomes suggest three ancestral populations for present-day Europeans. Nature. 513(7518):409–413. doi: 10.1038/nature13673.

Lipson M. 2020. Applying f4-statistics and admixture graphs: theory and examples. Mol Ecol Resour. 20(6):1658–1667. doi:10.1111/1755-0998.13230.

Massa M. 2016. Networks before empires: cultural transfers in western and central Anatolia during the Early Bronze Age [doctoral dissertation]. UCL (University College London) London, London, UK.

Patterson N, Moorjani P, Luo Y, Mallick S, Rohland N, Zhan Y, Genschoreck T, Webster T, Reich D. 2012. Ancient admixture in human history. Genetics. 192(3):1065–1093. doi:10.1534/genetics.112.145037.

Patterson N, Price AL, Reich D. 2006. Population structure and eigenanalysis. PLoS Genet. 2(12):e190. doi:10.1371/journal.pgen.0020190.

Peter BM. 2016. Admixture, population structure, and F-statistics. Genetics. 202(4):1485–1501. doi:10.1534/genetics.115.183913.

Peter BM. 2022. A geometric relationship of F_2, F_3 and F_4-statistics with principal component analysis. Philos Trans R Soc Lond B Biol Sci. 377(1852): 20200413. doi:10.1098/rstb.2020.0413.

Petr M, Pääbo S, Kelso J, Vernot B. 2019a. Limits of long-term selection against Neandertal introgression. Proc Natl Acad Sci U S A. 116(5):1639–1644. doi:10.1073/pnas.1814338116.

Petr M, Vernot B, Kelso J. 2019b. Admixr—R package for reproducible analyses using ADMIXTOOLS. Bioinformatics. 35(17):3194–3195. doi:10.1093/bioinformatics/btz030.

R Core Team. 2023. R: A Language and Environment for Statistical Computing. Vienna, Austria: R Foundation for Statistical Computing. https://www.R-project.org/.

Rodríguez-Varela R, Günther T, Krzewińska M, Storå J, Gillingwater TH, MacCallum M, Arsuaga JL, Dobney K, Valdiosera C, Jakobsson M, *et al.* 2017. Genomic analyses of pre-European conquest human remains from the Canary Islands reveal close affinity to modern North Africans. Curr Biol. 27(21):3396–3402.e5. doi: 10.1016/j.cub.2017.09.059.

Rogers AR, Bohlender RJ. 2015. Bias in estimators of archaic admixture. Theor Popul Biol. 100:63–78. doi:10.1016/j.tpb.2014.12.006.

Şahoğlu V. 2005. The Anatolian Trade Network and the Izmir region during the Early Bronze Age. Oxford J Archaeol. 24(4):339–361. doi:10.1111/j.1468-0092.2005.00240.x.

Skourtanioti E, Erdal YS, Frangipane M, Balossi Restelli F, Yener KA, Pinnock F, Matthiae P, Özbal R, Schoop U-D, Guliyev F, *et al.* 2020. Genomic history of Neolithic to Bronze Age Anatolia, Northern Levant, and Southern Caucasus. Cell. 181(5):1158–1175.e28. doi: 10.1016/j.cell.2020.04.044.

Skourtanioti E, Ringbauer H, Gnecchi Ruscone GA, Bianco RA, Burri M, Freund C, Furtwängler A, Gomes Martins NF, Knolle F, Neumann GU, *et al.* 2023. Ancient DNA reveals admixture history and endogamy in the prehistoric Aegean. Nat Ecol Evol. 7(2): 290–303. doi:10.1038/s41559-022-01952-3.

Slatkin M, Pollack JL. 2008. Subdivision in an ancestral species creates asymmetry in gene trees. Mol Biol Evol. 25(10):2241–2246. doi:10.1093/molbev/msn172.

The International HapMap Consortium. 2007. A second generation human haplotype map of over 3.1 million SNPs. Nature. 449(7164):851–861. doi:10.1038/nature06258.

Tricou T, Tannier E, de Vienne DM. 2022. Ghost lineages highly influence the interpretation of introgression tests. Syst Biol. 71(5): 1147–1158. doi:10.1093/sysbio/syac011.

Editor: K. Lohse